Multiphysics Design of a 130 GHz Klystron

Alberto Leggieri[1*], Davide Passi[1], Rocco Citroni, Giovanni Saggio[1] and Franco Di Paolo[1]
[1]Dept. of Electronic Engineering, University of Rome "Tor Vergata", Italy
*Corresponding author: alberto.leggieri@uniroma2.it

Abstract: The Multiphysics analysis of a 130 GHz klystron is described in this paper. Critical quantities are exposed to multiple physics effects acting on narrow dimensions modified by power dissipations. The proposed device uses an integrated injection/bunching section described in last COMSOL conference appointment. In order to stabilize electromagnetic beahvior in thermo-mechanical operative conditions, the system is based on carbon nanotube cold cathode and use an opportune airflow. Frequency shift in operative condition is reduced by means of an anisotropic thermal expansion that compensates cavity radius dilation induced by heating phenomena. The multiphysics design, performed on COMSOL, ensures the desired behavior in operative conditions.

Keywords: Electron Gun, Klystron, M Multiphysics Modeling,

1. Introduction

Klystrons are widely used vacuum tube amplifiers well suitable also as oscillators [1-2] that use electron beam through one or more resonant cavities where electron beam interacts with low energy alternate field. The beam in another cavity induces an oscillating field stronger than the first used for bunching resulting in an amplification of the signal. Interesting Klystron design techniques have been recently developed, allowing for the mechanical micromachining of 100 GHz Klystrons and photolithographic fabrication in the THz range [4-5].

Recently developed fabrication technologies have hallowed for the implementation of emitter cathodes on a micron scale, using the Photolithography suitable for miniature vacuum tubes [2]. Another Useful solution is the Micro-electro-mechanical systems (MEMS) fabrication, based on deep reactive-ion etching. The proposed device can be micro-fabricated by employing such techniques over a silicon wafer [3].

The Electron Gun (e-Gun) provides a small beam according to recent Millimetric devices [6]. The Cold cathode technology contributes to reduce thermal expansion typical of the classical thermionic cathodes.

This study shows the behavior of the miniature Klystron that experiences heating and power dissipations induced by wall current and electron gun dissipation. The Multiphysics modeling proposed in this paper is addressed to control temperature and thermal expansion by means of an opportune airflow. The device is composed by two cavities, Buncher and Catcher. The effect of the cathode heating on the Buncher was investigated in [3]: Typically if the cavity radius is increased, the resonance frequency decreases, if the cavity gap increases the frequency increase. An isotropic thermal expansion may dilate the cavity decreasing the operative frequency. For this aim, the surrounding temperature is decreased by airflow.

Mechanical constraint and possible direction of thermal expansions are considered while the airflow is oriented towards a certain direction for cooling off some surfaces more than others and inducing anisotropic thermal expansion. The main model is depicted in figure 1. The solid material is a block of Silicon at which interior, the vacuum region of electron gun and Buncher is present. A layer of Silver is deposed on the internal surfaces except for the circular lateral surface of the gun that insulates the anode to the cathode.

2. Use of COMSOL Multiphysics

In this paper a global analysis is reported where several factors have been considered simultaneously as mechanical stress, thermal expansion and fluid flow, together with the electromagnetic behavior of the device, through a Finite Element Method computation based on COMSOL. In the computational model, the geometry in figure 1 has been inserted inside a box where airflow has been prescribed with other

environmental conditions as temperatures and mechanical constraints.

An initial Electromagnetic (EM) analysis is used to compute the microwave power dissipations while the Buncher receive the operative input signal of 50 mW mean power at the input port and at the catcher output port the power produced by the device is prescribed. This power has been calculated by a traditional Klystron computation algorithm, AJ-Disk [7], developed at the Stanford Linear Accelerator Center (SLAC).

A Thermo-mechanical (TM) analysis is used to calculate temperatures and deformations considering the heating effects due to the power dissipations in the cavities superposed to that of the cathode, when heat flux has been diffused on all components, externally cooled by the airflow.

A Thermodynamic (TD) and Fluid Dynamics (FD) analysis have been coupled to a Solid Mechanics (SM) analysis obtaining temperature distribution and matrices of displacements. These displacements have been employed to produce a deformed geometry by Moving Mesh (MM) interface [8]. MM computation moved the mesh in function of the displacement found by the SM analysis. Electromagnetic calculation has been executed on the new meshes, receiving the stored temperatures. A diagram of the logical computation flow [3] is reported in figure 2.

2.1 Electromagnetic Waves

A cylindrical cavity with rectangular reentrant cross section with sharp edges has been employed. The cavity radius has been enlarged to match a standard WR-8 waveguide long side. The resonant magnetic field, used for bunching, oscillates in a quasi TM_{010} cylindrical cavity mode as the generated mode in the Catcher that provides energy to the output port. In the proposed study, a waveguide aperture is used for launching the field in cavity. A doubly tapered section proposed in [3] has been employed for the correct coupling of Buncher and Catcher with input and output waveguide ports respectively. Standard WR-8 waveguide flanges are available at the ports for the connection of low level signal and load respectively.

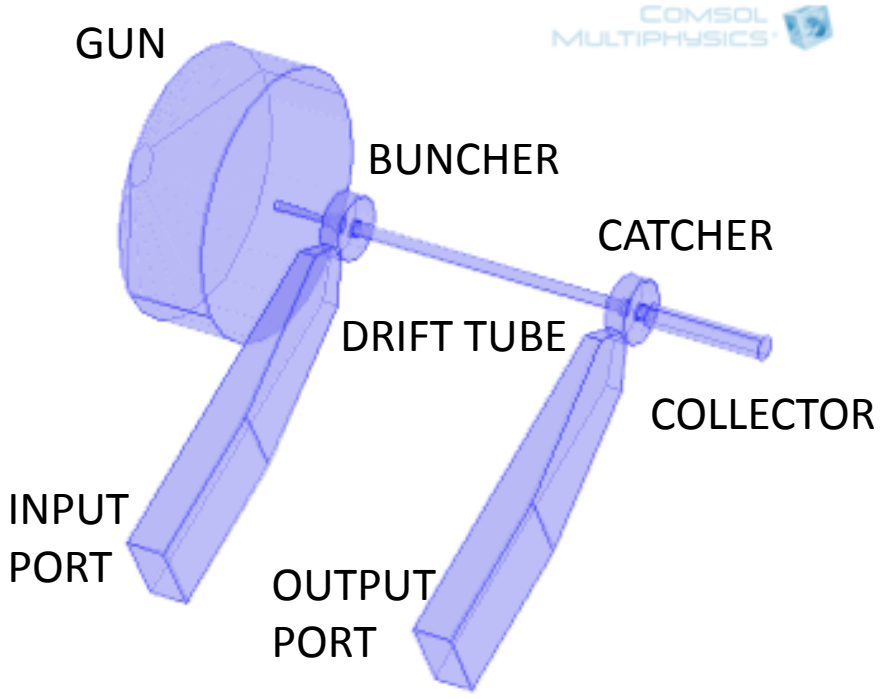

Figure 1. Electron gun connected to the Buncher

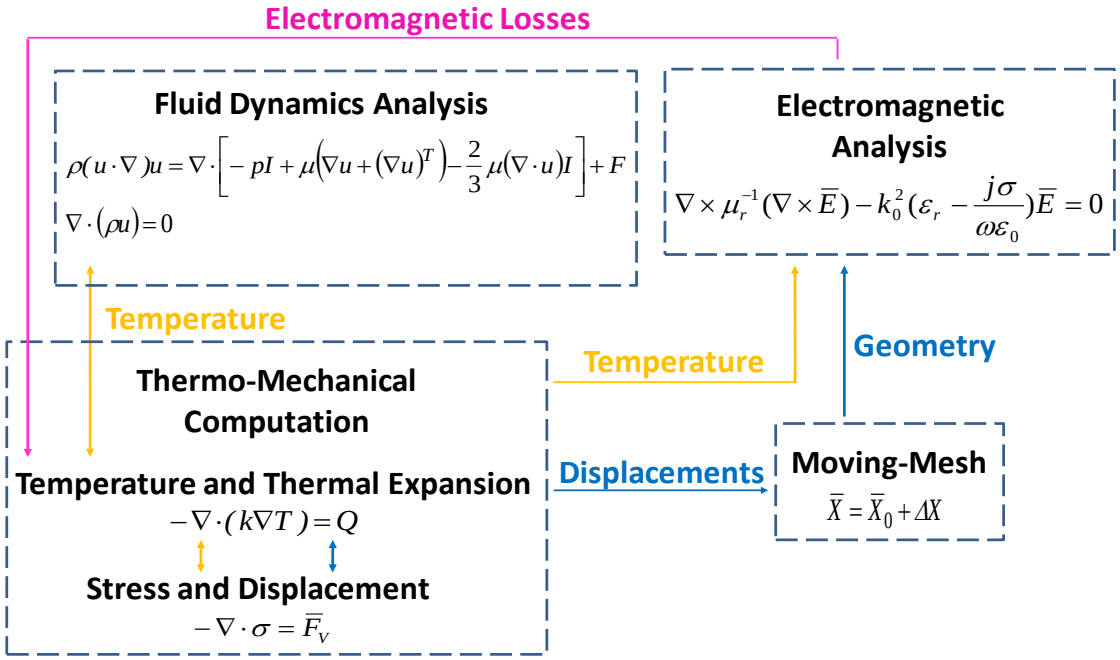

Figure 2. Computation Logical Diagram.

The analytical design of the cavities has been described in [3]. The Catcher is identical to the Buncher. Radii of cavities has been chosen to have a resonance around 130 GHz. For TM_{010} mode the radius of a cylindrical cavity is r_p = $2.405\lambda / (2\pi f) = 2.405c / (2\pi f)$ = 0.883 mm. The interaction gap has been dimensioned following accelerator design technique to maximize the shunt resistance over quality factor ratio R_s/Q. Cavity gap should be the 44% of the resonance wavelength, $L_g = 0.44\cdot\lambda$ = 1.015 mm.

The radius of the drift tube has been chosen, according to [7] without exceeding the 15% of the cavity radius. The drift tube radius has been set to $r_t = 0.14\cdot r_p$ = 0.124 mm. The analytical design of the cavity has been performed solving the system of equations described by Carter [3]. By referring to this nomenclature, we propose the following proportions for cavity dimensioning. Current values have been a bit modified to match the design frequency and truncate at the second significant factor (tenth of microns) and the following values have been obtained: $r_1 = r_t \approx 0.16$mm, $r_2 = 1.8r_t \approx 0.22$mm, $r_3 = 0.9r_p \approx 0.80$mm, $z_1 = 0.5L_g \approx 0.50$mm, $z_2 = 0.16L_g \approx 0.16$mm, $z_3 = 0.25L_g \approx 0.25$mm. The unperturbed analytical frequency of resonance is 132.32 GHz. By adopting particular cavity design techniques, based on higher order mode operation, the cavity dimensions can be further enlarged extending the realizability to frequency operation in the THz range [4-5].

The unperturbed analytical frequency of resonance of the cavities is 132.32 GHz. However, it has been demonstrated that higher order mode operation allows to extend the realizability to the THz range [4-5], but is not this case. We use a quasi-TM_{010} mode.

The electromagnetic analysis has been performed on the RF module of COMSOL Multiphysics to solve the wave equation in the frequency domain (1) [8].

$$\nabla\times\mu_r^{-1}(\nabla\times\bar{E})-k_0^2(\varepsilon_r-\frac{j\sigma}{\omega\varepsilon_0})\bar{E}=0 \qquad (1)$$

where μ_r is the relative magnetic permeability, ε_r the relative electrical permittivity and σ the electrical conductivity of the material ($S\cdot m^{-1}$); ε_0 is the electrical permittivity of the vacuum ($F\cdot m^{-1}$), k_0 the wave number in free space (m^{-1}), ω the wave angular frequency (s^{-1}) and $\bar{E}$ the electric field ($V\cdot m^{-1}$). The (1) has been computed by the Electromagnetic wave (EMW) feature with the following main boundary conditions [2]:

- Impedance boundary condition: The surfaces, shared between vacuum and the supporting solid material, are modeled in order to consider the losses due to the partial penetration of the electric field in the lossy material which constitutes such walls. The specified thickness of the wall boundaries is fixed to 80μm.
- Rectangular ports: In order to allow EM energy enters or exits the cavities to and from waveguides, rectangular ports have been used. The input port is set to launch and the TE_{10} mode of a rectangular waveguide. The average power input is 50 mW. At the output port, a power of 2W, calculated by AJ-Disk [7] has been prescribed.

All the cold parameters of the cavity and the total power dissipation have been calculated in this step and stored in memory.

The Smith chart over the Nyquist plot is reported in figure 3 to show the power coupling by means of the resonance circle [3] that approaches to the unitary circle, showing a critical coupling.

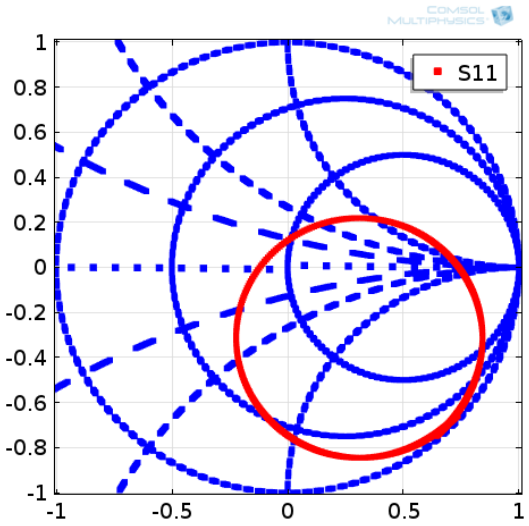

Figure.3. Smith Chart represented over the Nyquist plot. The Resonance circle is superposed to evaluate the coupling.

The carbon nanotube (CNT) cathode can be developed by existing micromachining and photolithography processes and has been designed by following the theory reported in [9] consistently with vacuum devices already studied in millimeter and sub-millimeter frequency range [6]. At ambient temperature (20°C), the cathode reaches 35°C and produces a 16 mA beam of 10 keV electrons that is injected at the Buncher interface [3].

2.2 Heat Transfer and Fluid Flow

In this step, TD and FD analysis [10] are coupled. Fully coupled stationary calculation has been used for the evaluation of temperature distribution at the steady state, when the cathode temperature and cavity dissipations are fixed at operative values and the structure is subjected to the air flow of 2 ms^{-1} velocity normally oriented towards the lateral surface where is not present the input flange.

Heat Transfer (HT) module of COMSOL has been used to solve the Heat Equation in the steady state (2) [8].

$$-\nabla\cdot(k\nabla T)=Q \qquad (2)$$

where k is the thermal conductivity ($W\cdot m^{-1}\cdot K^{-1}$) of the material and Q is the heat power density (Wm^{-3}). The power dissipation calculated in the previous Electromagnetic analysis has been prescribed on the Buncher walls as surface density power source, introducing another equation similar to (2) where the ∇ operator is replaced by a normal unitary vector and k has the negative sign ahead and the heat power density is given by the total electromagnetic losses.

The HT module has been set up with the following main boundary conditions:
- Heat transfer in Fluids: The non ideal vacuum and the air atmospheres inside the gun and Buncher volume are modeled only to describe the heat transfer and excluded from moment computations.
- Temperature: The temperature of the wall where the air flux enter inside the volume used to calculate the air flow (the air box) is set to the external temperature, fixed to T_{ext} = 20°C, consistently with a typical environment temperature condition. Another boundary condition is prescribed to the cathode surface, since it operates at 35°C.
- Heat source: The interior volume of the Buncher is a volume heat source defined through the total power dissipation density previously computed by a preliminary EM analysis computed as a first step.

The air motion is modeled with a single phase laminar flow and computed by solving the system of (3) and (4) in a stationary analysis [10] inserting the Laminar Flow (LF) feature of COMSOL.

$$\rho(u\cdot\nabla)u = \nabla\cdot\left[-pI+\mu\left(\nabla u+(\nabla u)^T\right)-\frac{2}{3}\mu(\nabla\cdot u)I\right]+F \quad (3)$$

$$\nabla\cdot(\rho u)=0 \quad (4)$$

where p is the pressure, u is the velocity field ($m\cdot s^{-1}$), the material density ($kg\cdot m^{-3}$), μ the dynamic viscosity ($Pa\cdot s$) of the material (the air) and F is the volume force ($N\cdot m^{-3}$). The symbol I stand for the identity matrix and T for the transposing operation. The LF computation has been performed including the following main boundary conditions:

- Inflow: The shortest side of the volume where the device is immerged has a boundary condition which imposes the input of the cooling airflow.
- Outflow: The opposite shortest side of the volume mentioned above has a boundary condition imposing the output of the cooling air flux.

No Symmetry conditions are used in this second design step because the whole device has been simulated. In the previous step, described in [3], the preliminary design of the system was performed including the gun and the Buncher. I that case, the widest side of the air box volume, where the device is immerged, had a boundary condition stating the symmetry with the corresponding opposite face.

2.3 Solid Mechanics Analysis

Concurrently with previously described computations, the SM module received the output temperature and calculated thermal displacements. Surfaces are in a stationary thermal regime, cooled by the external air flow. The stress steady state equation (5) has been solved fully coupled with the (2), (3) and (4) by computing thermal expansion [8].

$$-\nabla\cdot\sigma=\overline{F}_V \quad (5)$$

where σ is the stress (Nm^{-2}) and $\overline{F}_V$ is the force per unit volume (Nm^{-3}). The main boundary condition of this step is the fixed constraints: The external walls are free to move, except for the face where the cathode is mounted. This is modeled as fixed constraint because the device is supported from this face by the cathode assembly. The solid model is isotropic with quasi-static structural transient formulation.

2.4 Moving Mesh

After the HT, LF and SM analysis, the MM dedicated interface has been employed to produce deformed meshes in function of the displacements. Deformed meshes are used for the computation of the electromagnetic behavior. In the MM interface, the following features have been used [4]:

- Prescribed deformation: The structure of the gun and Buncher represent the volume subjected to deformation. The displacement vectors (u, v, w) computed by the SM module are employed to specify this volumetric deformation. Its prescribed mesh displacement is set to $d_x= u$, $d_y=v$, $d_z=w$.
- Free deformation: The non ideal vacuum and air volumes (which are not subjected to any structural elastic formulation by the SM analysis) are free to move. Initial deformation is set to $dx_0=0$, $dy_0=0$ and $dz_0=0$.
- Prescribed Mesh Displacement: This condition specifies that the surface boundaries shared between the volumes subjected to deformation and the ones free to move need to be deformed by the SM computation. This allows the free volume to follow the deformation of the volumes deformed by the SM step, though is attached to the free deformation air and non ideal vacuum boundaries. Such surfaces are subjected to deformation. This superficial displacement has been specified by setting the prescribed mesh displacement to $d_x= u$, $d_y=v$, $d_z=w$.

After this study, new mesh configuration has been produced. In the solution related to the MM study, by re-mesh deformed configuration. A “deformed configuration” sub-node appeared in the “Mesh” node on the model three. In such sub-node, has been asked to “build all”. New meshes have been produced.

3. Thermomechanical Features

The airflow performs the device cooling as shown in fig 4, where the external maximum temperature approaches to 34.8°C. As shown in figure 5, the maximum temperature reached by the system is 35°C. In order to underline the deformation, stress and displacement are been plotted with a magnified scale. In the following figures, black outlines represent the original conformation, and the stained volume represents the deformed structure. As cold condition, the case of the sole EM computation is intended without Multiphysics computation. As thermomechanical operative condition, the concurrent action of both cathode heating and the cooling airflow at the same time is intended.

The global temperature distribution has induced a maximum stress of about 23.1 MNm^{-2} (figure6) located at the interfaces between the warmest face which is fixed to the rigid support. The internal shape, more free to deform, is less stressed than this interface. The maximum total displacement is located on the face where no fixed constraints are present and is about 1.36 μm (figure 7). This low dilation is allowed by the low thermal expansion of silicon.

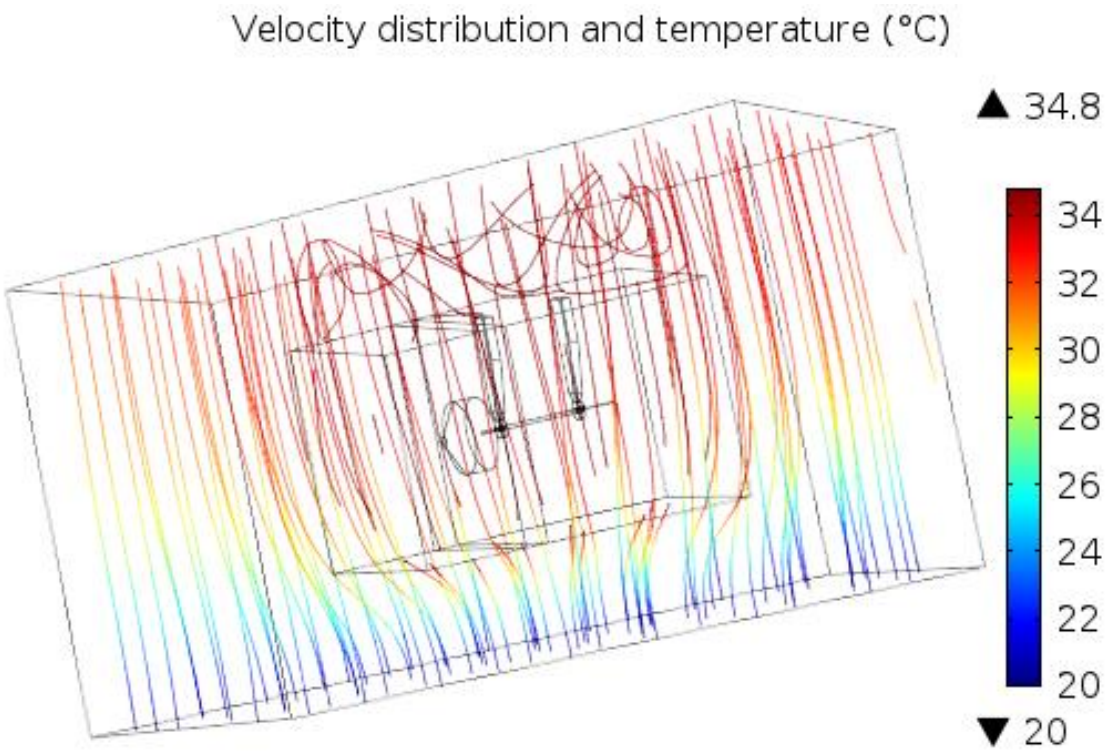

Figure 4. Airflow path with temperature distribution (°C).

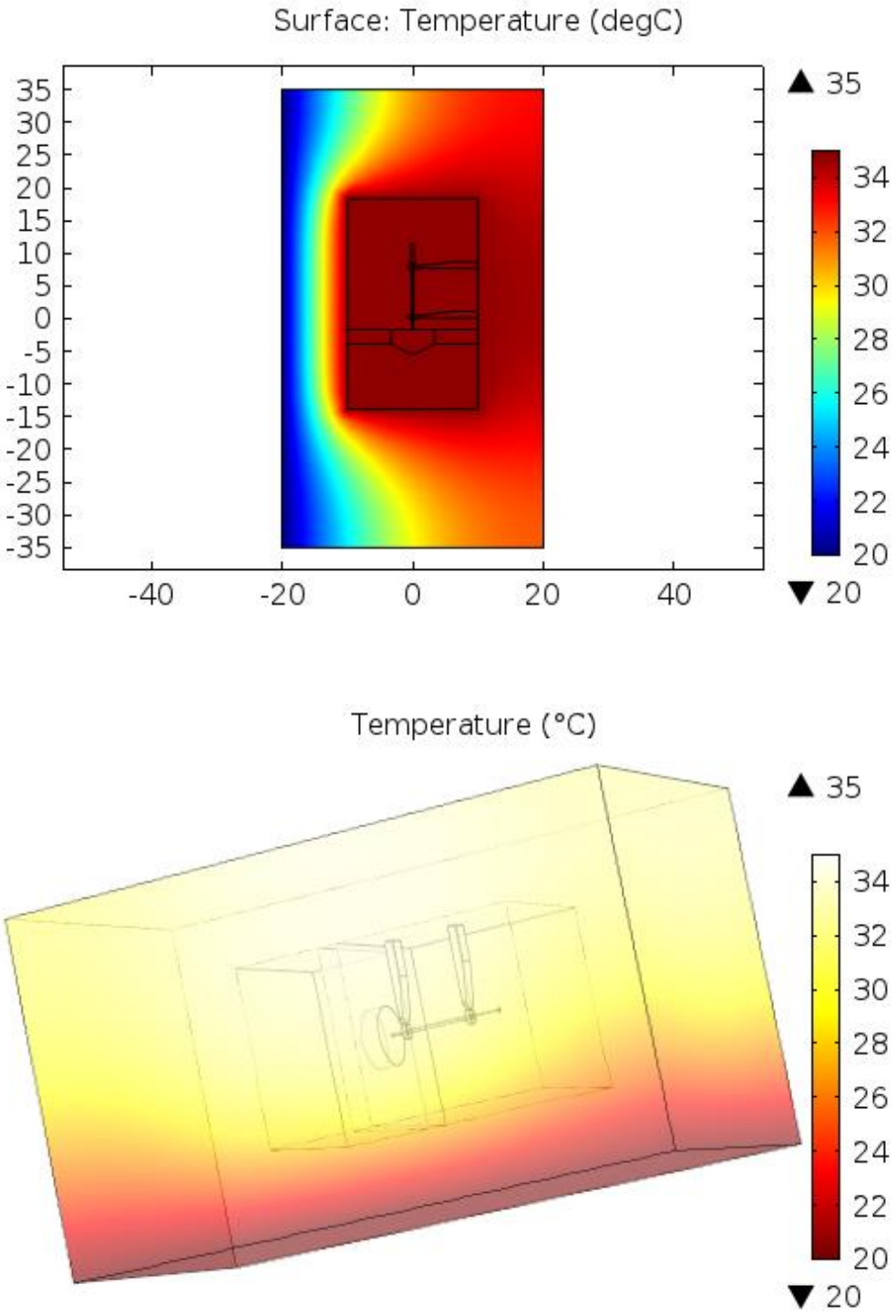

Figure 5. Temperature (°C): Cross sectional (upper) and external 3D (lower) views.

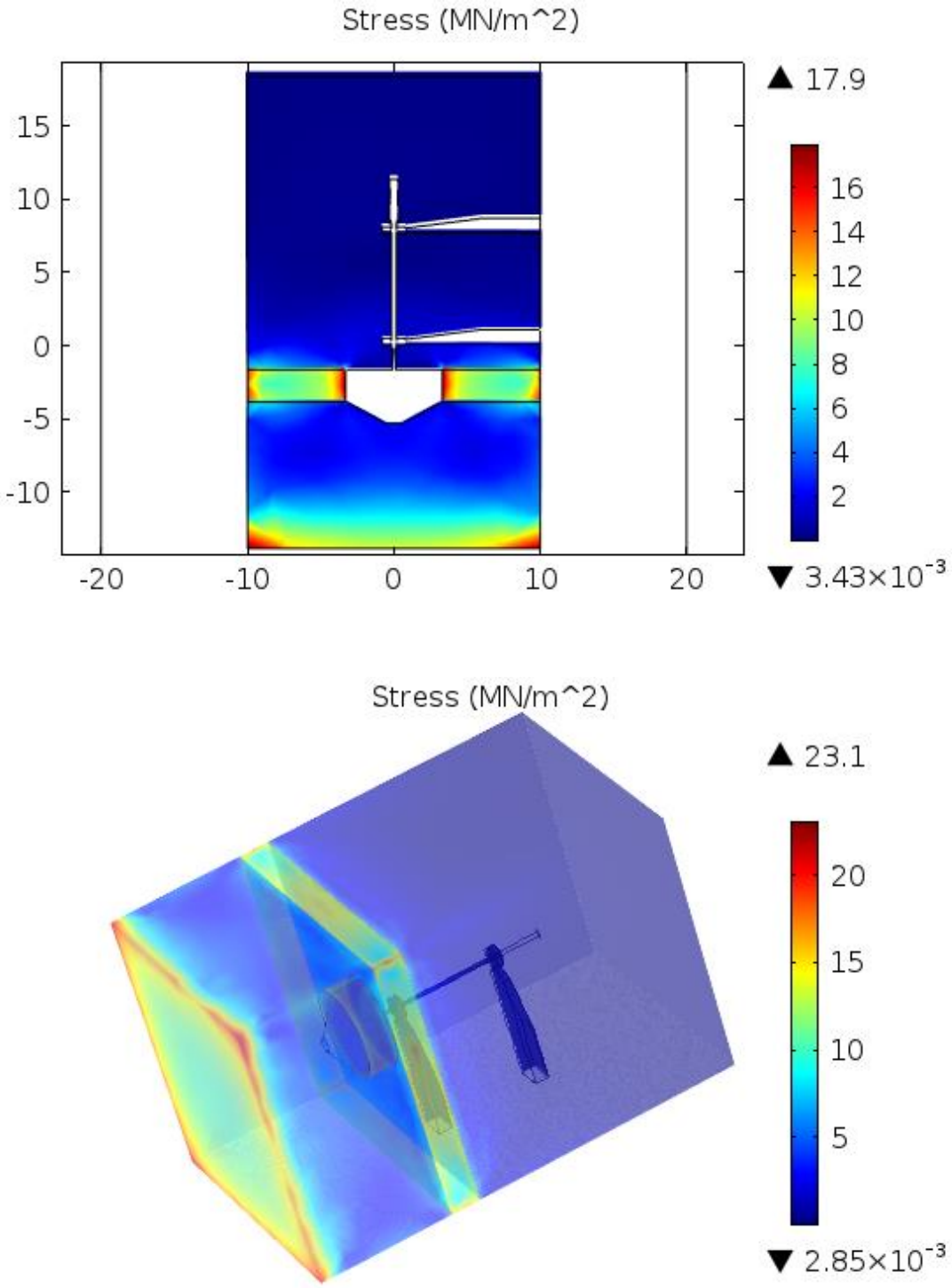

Figure 6. Stress (kNm^{-2}): Side (upper) and 3D (lower) views.

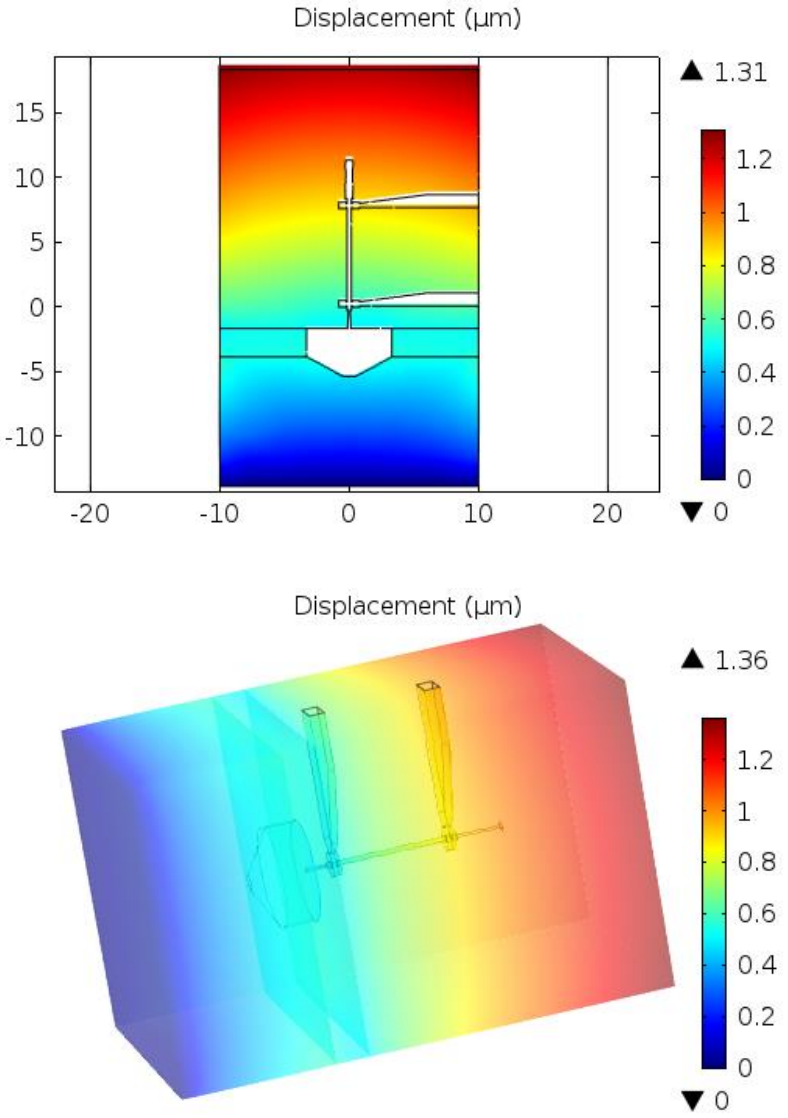

Figure 7. Displacement (μm): Side at center (upper) and 3D (lower) views.

4. Electromagnetic Features

The EMW analysis has given the following results. The scattering parameters in cold and in TM operating conditions have been documented and reported in figure 8.

In this analysis has been considered also the case of the sole computation of thermal condition without considering thermomechanical induced deformation. As shown in the yellow curve of figure 8, the resonance frequency of the Buncher from the cold condition (where it has the value of f_1=131.68 GHz, blue curve) decreases to f_2 = 131.67 if only the thermodynamic condition is considered. The same value is obtained for the Catcher cavity as shown in cyan curve. By considering thermomechanical displacement, the frequency is increased due to the gap dilation. In this condition, the Buncher resonance frequency moves to f_3=131.69, as shown in the red curve of figure 8, while the Catcher frequency remains at 131.68 GHz as shown in green curve. This is a very good result. Reason of this behavior resides in the gap dilation phenomena: While the cooling air flux is operating, the controlled temperature at cavities lateral surfaces contains

shape alteration. Anyhow, the base surface, where the beam crossing hole is located, cavity tends to expanse straightly, since it is less refrigerated, due to the positioning of the air flux streamlines which are crossed to longitudinal axis. This effect allows for a frequency increase.

The insertion loss of the Buncher increases from 18.6 to 19.6dB but the insertion loss of the Catcher decrease from 19.4 to 18.0 db. This is a very small disadvantage. This effect is dependent of the external shape which cannot modify the field in cold conditions but is determinant in operative conditions. It's evident as an opportune exterior shape can re-increase the performance of the device while it undergoes the operative influencing factors.

In figure 9 we can observe the streamline distribution of the electrodynamic fields in the cavities. While receiving 50mW at the input, the axial electric field inside the Buncher reaches a maximum m value of E_{ACmax} = 0.35 MVm^{-1} in cold condition and E_{ACmax} = 0.36 MVm^{-1} thermo-mechanical operating conditions. However, at the center of the cavity it decrease slightly from $E_{AC(r=0)}$ = 0.35 MVm^{-1} (that, in this case, it corresponds with the maximum amplitude in the Buncher) to $E_{AC(r=0)}$ = 0.27 MVm^{-1} in thermomechanical condition, as shown in fig. 10. In this image, longitudinal distributions of electrodynamic fields at the cavity centers are reported.

While producing 2 W output power, the Catcher reaches in cold conditions E_{ACmax} = 0.65 MVm^{-1} and in thermo-mechanical operating conditions E_{ACmax} = 0.89 MVm^{-1} (figure 9) but at the center of the Catcher, from $E_{AC(r=0)}$ = 0.65 MVm^{-1} it becomes $E_{AC(r=0)}$ = 0.68 MVm^{-1} (figure 10).

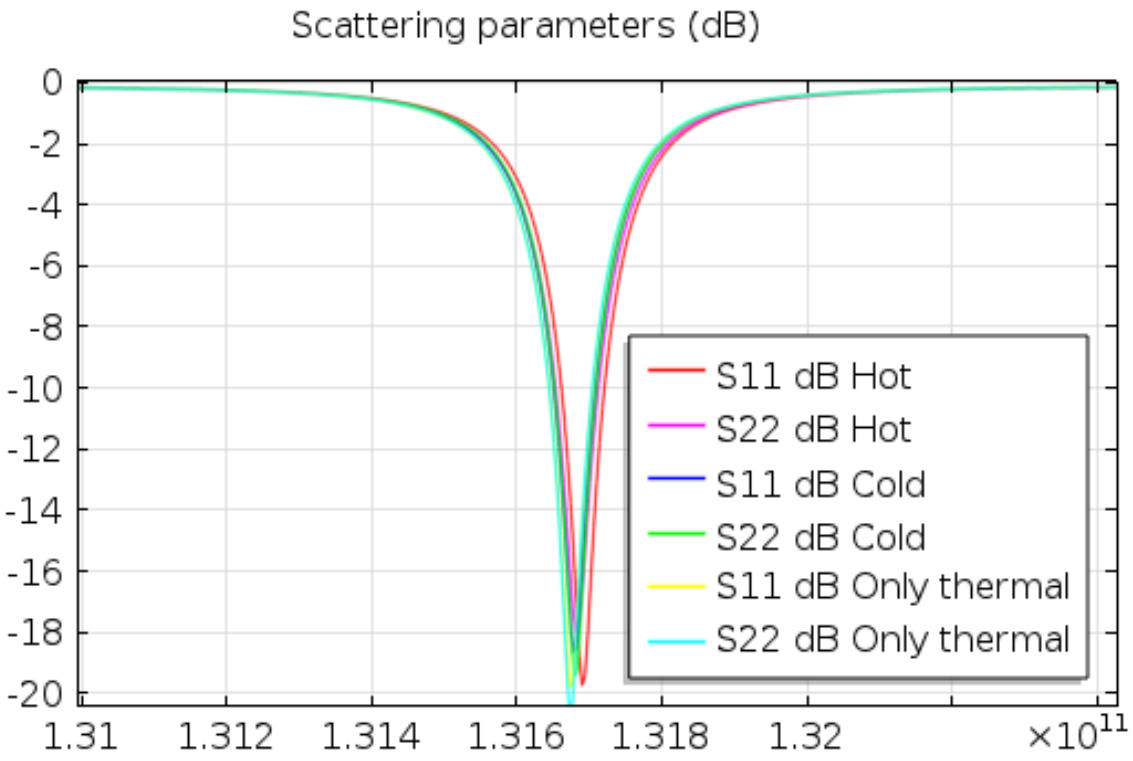

Figure 8. Scattering refection parameter S_{11} in dB: Cold and working conditions considering cooling airflow.

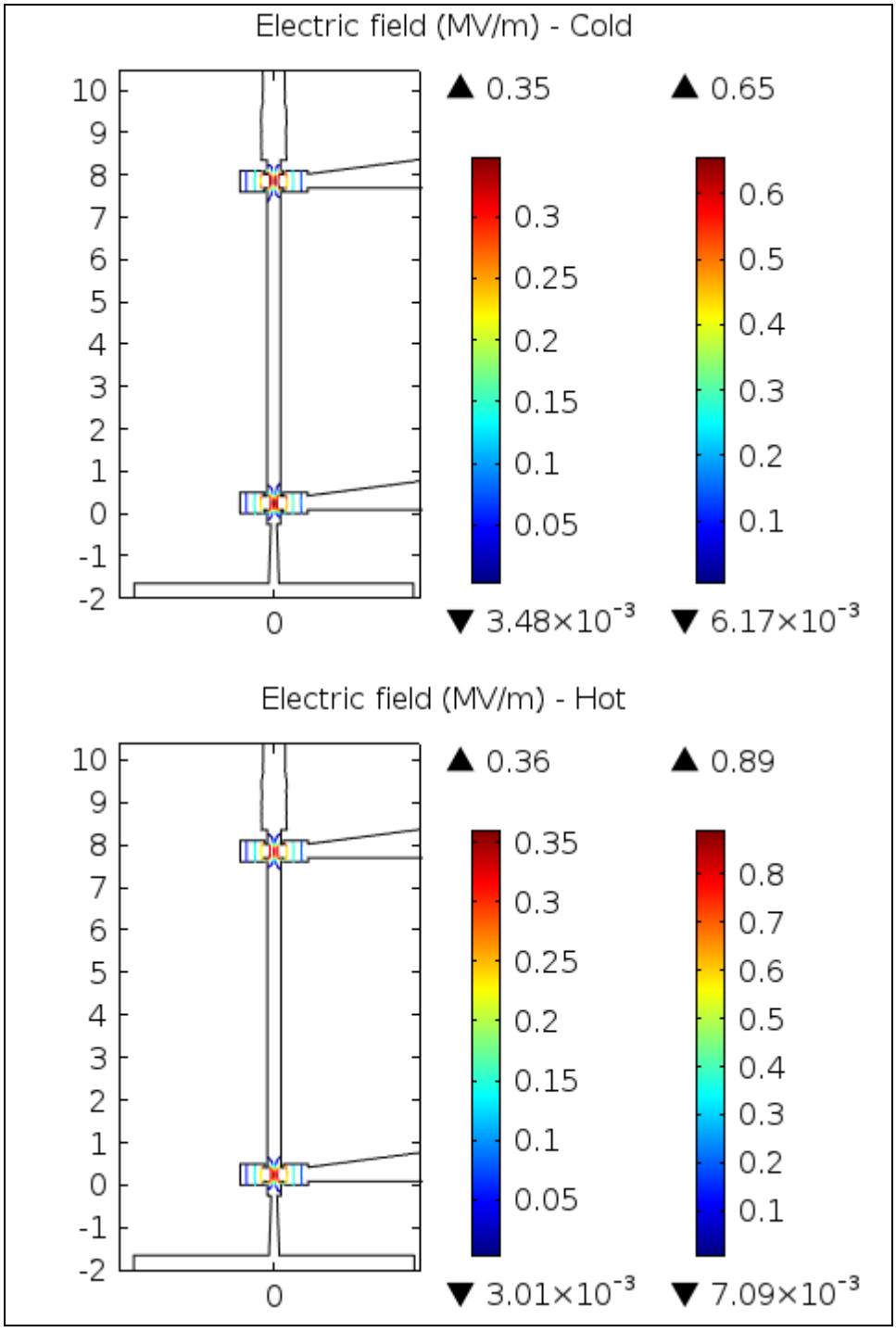

Figure 9. Distribution inside cavities of the electrodynamic fields MVm^{-1}: Cold and (left) working conditions (right).

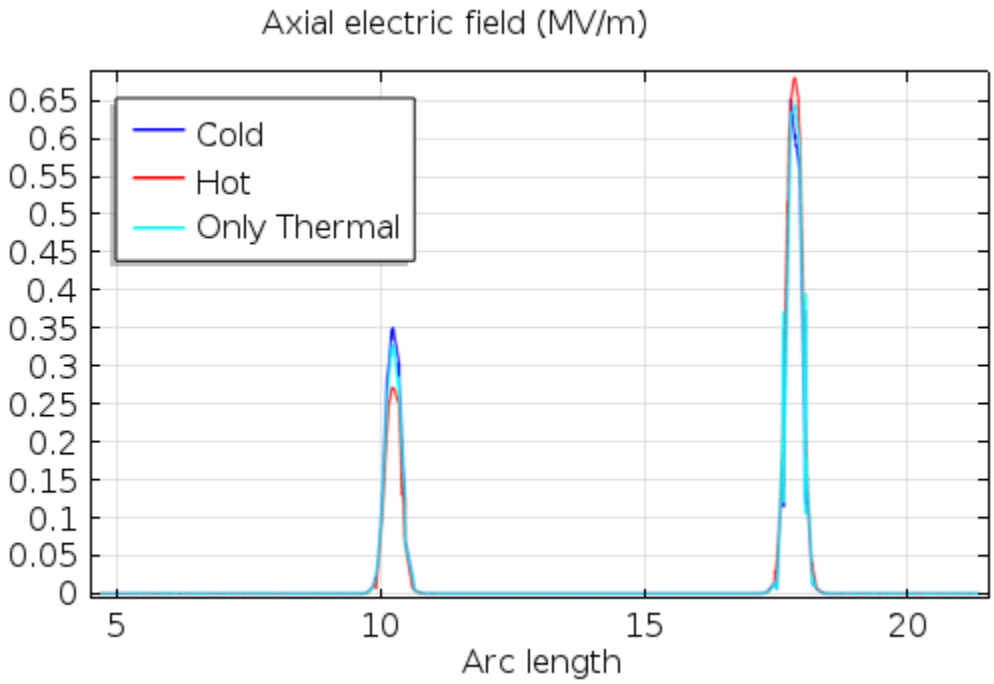

Figure 10. Axial electric field at cavity center (MVm^{-1}): Cold and working conditions, considering frequency shift.

5. Conclusions

In this paper, Multiphysics analysis of a 130 GHz klystron is shown. The discussion is focused on the modification to the electromagnetic behavior induced to alterations of critical quantities dependent on thermomechanical exposition.

A miniature 130 GHz Klystron is proposed. It uses the integrated injection/bunching section described in last COMSOL conference appointment [3]. The system is based on carbon nanotube cold cathode and opportune airflow to control the temperature. The multiphysics design is performed on COMSOL in order to ensure the desired behavior in operative conditions

In order to control thermomechanical effects as heating and power dissipations, an air flow has been used to control the temperature. The Carbon nanotube cold cathode allows operating at 35°C of temperature.

A multiphysics design on COMSOL Multiphysics have allowed for the computation of a Thermo-mechanical analysis by coupling Heat Transfer, Solid Mechanics and Laminar Flow modules. Temperatures and deformations have been determined, when the heat produced internally has been diffused to the whole system. Thermo-mechanical displacements have been computed and the Moving Mesh (MM) dedicated interface has been used to obtain the deformed geometry, where electromagnetic analysis is performed. Scattering parameters at the input and output porta and axial electric field of the cavities have been calculated. The requirements for the air flow have been estimated.

This study shows the advantage of using cold cathode and cooling airflow, in order to reduce undesired thermal effects in miniature Klystrons.

Several strategies have been adopted to obtain a simple but reliable model. The proposed approach has allowed selecting the appropriate materials and geometries.

9. References

1. D. Passi, A. Leggieri, F. Di Paolo, M. Bartocci, A. Tafuto, A. Manna, “High Efficiency Ka-Band Spatial Combiner”, *Advanced Electromagnetics*, Vol. 3, No. 2, page 10-15 (2014).

2. P.H. Siegel, A. Fung, H. Manohara, J. Xu, B. Chang, "Nanoklystron: A Monolithic Tube Approach to THz Power Generation". *Proc. of the Twelfth International Symposium on Space Terahertz Technology*, February 14-16, Shelter Island, San Diego, CA, USA, (2001).
3. A. Leggieri, D. Passi, G. Saggio and F. Di Paolo, "Multiphysics Design of a Klystron Buncher", Proc. of COMSOL Conference 2015 Grenoble (2015).
4. M. Mineo and C. Paoloni, "Micro Reentrant Cavity for 100 GHz Klystron", *Proc. of IEEE Vacuum Electronics Conference (IVEC)*, Monterey, CA, 2012, page .65-66 (2012).
5. C. Paoloni, M. Mineo, H. Yin, L. Zhang, W. He, C.W. Robertson, K. Ronald, A.D.R. Phelps and A.W. Cross, "Scaled Design and Test of a Coupler for Micro-Reentrant Square-Cavities for Millimeter Wave Klystrons", *Proc. of IEEE Vacuum Electronics Conference (IVEC)*, Paris, 2013, page 1-2 (2013).
6. A. Leggieri , G. Ulisse, F. Di Paolo, F. Brunetti, A. Di Carlo, "Particle tracing simulation of a vacuum electron gun for THz application", *Proc. of IEEE Millimeter Waves and THz Technology*, Rome (2013).
7. G. Caryotakis, "High Power Klystrons: Theory and Practice at the Stanford Linear Accelerator Center" SLAC-PUB 10620, 2005, pp.34-35.
8. A. Leggieri, D. Passi, F. Di Paolo, "Key-Holes Magnetron Design and Multiphysics Simulation", *Proc. of COMSOL Conference 2013*, Rotterdam, NL (2013).
9. J. R. Pierce, *Theory and Design of Electron Beams*, D. Van Nostrand Company, Canada, The Bell Telephone Laboratories Series (1949).
10. COMSOL, *Heat transfer Module User's Guide*, COMSOL AB, Stockholm, page 69-72,111-212 (2012).